

# Shell model based deformation analysis of light Cadmium isotopes

T. Schmidt,<sup>1</sup> K. L. G. Heyde,<sup>2</sup> A. Blazhev,<sup>1</sup> and J. Jolie<sup>1</sup>

<sup>1</sup>*Institut für Kernphysik, Universität zu Köln, Germany*

<sup>2</sup>*Department of Physics and Astronomy, Ghent University, Belgium*

(Dated: October 25, 2018)

Large-scale shell-model calculations for the even-even Cadmium isotopes  $^{98}\text{Cd}$  -  $^{108}\text{Cd}$  have been performed with the ANTOINE code in the  $\pi(2p_{1/2}; 1g_{9/2}) \nu(2d_{5/2}; 3s_{1/2}; 2d_{3/2}; 1g_{7/2}; 1h_{11/2})$  model space without further truncation. Known experimental energy levels and  $B(E2)$  values could be well reproduced. Taking these calculations as a starting ground we analyze the deformation parameters predicted for the Cd isotopes as a function of neutron number  $N$  and spin  $J$  using the methods of model independent invariants introduced by K. Kumar and D. Cline.

## I. INTRODUCTION

In nuclei with a single closed shell (either protons or neutrons) the energy spectra are characterized by the pairing energy of the valence particles in the open shell, making seniority an approximate quantum number. For e.g., the Sn ( $Z = 50$ ) and Pb ( $Z = 82$ ) isotopes and the  $N = 82$  isotones this turns out to be the case. The pair-breaking energy (energy gap  $2\Delta$ ) separates the ground state from a rapidly increasing level density at energies of  $E_x \sim 1.5 - 2$  MeV. Moreover, the excitation energy of the first excited  $2^+$  state stays remarkably constant with changing neutron (in the  $Z = 50$  and  $Z = 82$  isotopes) or proton number (in the  $N = 82$  isotones). Pairing was incorporated using the BCS theory of superconductivity as applied to even-even atomic nuclei [1] and is described in detail by [2, 3]. This pairing fingerprint is well-covered by many present-day large-scale shell-model calculations [4, 5].

A few valence particle (or holes) away from the closed shell an onset of quadrupole collectivity appears, which is indicated by the change in excitation energy of the low-lying  $2_1^+$ ,  $4_1^+$ ,  $6_1^+$ , ... states as well as by the increase of corresponding  $B(E2)$  values. This is an interesting issue to explore in detail how nuclei with just two protons outside the closed shell (or missing) behave, see, e.g., the Cd ( $Z = 48$ ), Te ( $Z = 52$ ), the Hg ( $Z = 80$ ) and the Po ( $Z = 84$ ) isotopes, as well as isotones with  $N = 80$  and  $N = 84$ .

For the Cd nuclei, an extensive set of experimental data has been obtained over the years, covering essentially the whole  $N = 50 - 82$  neutron major shell, and even going beyond the  $N = 82$  closed shell, both on low- and high-spin states,  $B(E2)$  values, g-factors (see the detailed set of references: [6–64]), as well as the systematics for those data (see refs. [65–67]). See also reference [68] for a recent review on the structure of  $^{100}\text{Sn}$  and neighboring nuclei including the light Cd isotopes.

The Cd nuclei have been studied using shell-model calculations for the lighter mass region [7–12, 14, 18, 69] and also using the Interacting Boson Model (IBM) [17, 18, 21, 23, 51, 64, 70–77]. Besides that, other studies, starting from a general collective Bohr Hamiltonian, derived from a microscopic starting point using a Skyrme

force, calculations using the Adiabatic Time-Dependent Hartree-Fock-Bogoliubov (ATDHFB) method (for the nuclei  $^{106-116}\text{Cd}$ ) [78], as well as using a self-consistent HFB approach, starting from the finite range Gogny interaction [79] have been carried out.

Our aim, in the present paper, is to show how, starting from an extensive and large-scale shell-model calculation, it becomes possible to characterize the onset of quadrupole collectivity with increasing number of valence neutrons outside of the  $^{88}\text{Sr}_{50}$  core nucleus. We concentrate on the calculation of both quadratic and cubic rotational invariants (constructed starting from the  $E2$  transition and diagonal matrix element) as was originally proposed by Kumar [80] and Cline and Flaum. [81–84]. Subsequently, using those matrix elements as input, we can extract quantitative information about the changing collective properties of the low-lying states (band structure if possible), through the quadrupole parameters ( $\beta$ ,  $\gamma$ ) [85], mainly used to characterize the intrinsic deformation properties of the Cd nuclei studied in the present paper.

The detailed spectroscopic results for the Cd nuclei, studied in this paper, such as energy spectra (covering both the low-spin and high-spin regions), indications of “collective bands” and related electromagnetic properties (mainly electric quadrupole and magnetic dipole), as well as a detailed comparison with the extensive set of data, will form the content for a forthcoming paper.

## II. SHELL MODEL CALCULATIONS

Large-scale shell-model calculations (LSSM) of Cadmium isotopes have been performed using the complete neutron model space ( $N = 50 - 82$ ), i.e. filling the  $2d_{5/2}$ ,  $3s_{1/2}$ ,  $2d_{3/2}$ ,  $1g_{7/2}$  and  $1h_{11/2}$  orbitals with neutrons while ten protons remain distributed in the  $2p_{1/2}$  and  $1g_{9/2}$  orbitals ( $Z = 48$ ) forming the proton model space ( $Z = 38 - 50$ ). This way  $^{88}\text{Sr}$  acts as an inert model space core, i.e. we assume no interaction between the valence particles in the model space and the inert core. Within this model space we study and explore a multitude of nuclear structure properties. In particular, the changing quadrupole collective properties, indicated through the

$E_x(2_1^+)$  and  $B(E2)$  values along the yrast band, with increasing number of valence neutrons moving outside the  $N = 50$  closed shell. The nucleon-nucleon interaction used is an effective realistic force originating from the Bonn-CD potential, resulting in a G-matrix called the  $v3sb$  effective interaction (see [12] page 2, left column for more details). This interaction has been modified implying a slight adjustment of the monopoles such as to exhibit the correct propagation of the single-particle neutron energies moving from  $N = 51$  ( $^{89}\text{Sr}$ ) towards the end of the shell at  $N = 81$  ( $^{131}\text{Sn}$ ) as well as some changes in the effective pp, np and nn matrix elements as outlined in ref. [12] resulting from a fit of the force to 189 data points (excitation energies) in the mass region considered here. This interaction is called later on  $v3sbm$ .

An important point is the right choice of the proton and neutron effective charges throughout the full set of Cd nuclei. The procedure used is to fix the proton effective charge  $e_\pi$  fitting the theoretical  $B(E2)$  value for the  $8_1^+ \rightarrow 6_1^+$  transition to the known experimental value in  $^{98}\text{Cd}$  [8]. Having fixed this value, the neutron effective charge  $e_\nu$  was fixed by comparing the experimentally known and theoretically calculated  $B(E2)$  values for the  $2_1^+ \rightarrow 0_1^+$  transitions in  $^{102,104}\text{Cd}$  [13]. The effective charges used in the current work are  $e_\pi = 1.7e$  and  $e_\nu = 1.1e$ , i.e., the same effective charges as in the previous shell-model calculations with this interaction [12, 13]. A former shell-model study on light Cd isotopes using  $v3sb$  by A. Ekström et al. [14] (see also references [86–88]) successfully reproduced the experimental values with similar effective charges.

With these ingredients kept constant in the LSSM study of the Cd nuclei, it is only the  $NN$  interaction acting in the large model space that produces the nuclear structure properties as a function of increasing neutron number. The large-scale shell-model calculations were performed with the code ANTOINE [4]. The calculations presented here were conducted in the full model space without any additional truncations. The m-scheme matrix dimension for  $m = 0$  in  $^{108}\text{Cd}$  was about  $10^8$ . First results have been published in [89].

### III. SHAPE INVARIANTS

It turns out that rather than comparing a multitude of experimental data separately with the results from a specific model description of nuclear structure, almost model-independent methods have been developed to characterize the nuclear quadrupole properties for all states. This leads to the possibility to find sets of correlated states based on the intrinsic properties for those states. The idea is to construct so-called rotational invariants, which, in the case of studying quadrupole collective properties, are built from a product of a number of the E2 operators [80, 81] which, starting from the E2

operator,

$$P_{2\mu} = \sum_{i=1}^A e_i r_i^2 Y_{2\mu}(\Omega_i), \quad (1)$$

is described as a tensor product of  $n=2,3,\dots$  such operators, coupled to a rank 0 tensor, defined as

$$P^{(n)} = [P_2 \otimes P_2 \otimes \dots \otimes P_2]_2 \cdot P_2. \quad (2)$$

When calculating the expectation value of such operators in any given eigenstate of the nucleus  $|J, M\rangle$  and because of its zero rank character, this gives rise to a rotational invariant quantity. As the spectroscopic quadrupole moments for  $0^+$  states vanish, invariants are also the only access to study the deformation of those states. This also implies that the results will be the same, independent of the reference frame used: be it the laboratory frame or the frame centered on the principal axis of the nucleus. For a more general derivation and discussion of these invariants, the reader is referred to the references [80, 81].

In this section, we give a short review on the building of these invariants and also lay open some differences in the methods initiated by Kumar [80] and Cline [81].

For our analysis, we aim to extract the deformation parameters  $\beta$  and  $\gamma$  as introduced by Bohr and Mottelson [85]. Therefore, it is sufficient to derive the invariants  $P_s^{(2)}$  and  $P_s^{(3)}$ , though invariants of higher couplings are possible in principle [81], denoted as  $P_s^{(n)} = \langle s, M_s | P^{(n)} | s, M_s \rangle$ , resulting in the expressions

$$P_s^{(2)} = \frac{1}{2I_s + 1} \sum_r (M_{sr})^2, \quad (3)$$

$$P_s^{(3)} = -\frac{\sqrt{5}}{2I_s + 1} (-1)^{2I_s} \sum_{rt} \left\{ \begin{matrix} 2 & 2 & 2 \\ I_s & I_r & I_t \end{matrix} \right\} M_{sr} M_{rt} M_{ts}, \quad (4)$$

with  $r$  and  $t$  describing the intermediate states of the coupling and with  $\left\{ \begin{matrix} 2 & 2 & 2 \\ I_s & I_r & I_t \end{matrix} \right\}$  denoting a Wigner-6j-symbol. Furthermore,  $M_{sr} = \langle s || P_2 || r \rangle$  is a shorthand notation for the reduced E2 matrix elements that are needed as input to calculate the  $P_s^{(2)}$  and  $P_s^{(3)}$  invariants. These can be the results extracted from experimental studies, or, as we are performing LSSM calculations for the Cd nuclei, the calculated E2 reduced matrix elements. In the above,  $s, r, t, \dots$  are shorthand notations to specify all quantum numbers necessary to characterize the various nuclear levels.

Once the invariants are calculated and available, deformation parameters can be extracted using methods originally proposed by Kumar [80] and Cline and Flaum ([81–84]) using slightly different methods to do so. These methods have been used in a large number of recent papers (in particular in the region of the Ge, Kr, Mo, Ru and Pd nuclei [90–95], as well as in the much heavier Pb mass region (W, Os, Pt, Hg, Po isotopes) [96–101].

In the present paper, we use both methods to study the sensitivity of the extracted deformation parameters  $\beta$  and  $\gamma$ , which we review in a succinct way so as to point out similarities and some subtle differences.

Shape invariants have also been studied within the context of the Interacting Boson Model (IBM) in various mass regions (see e.g. [102, 103] and references therein) in order to extract information on a mean-field level (nuclear quadrupole deformation parameters,..). Care should be taken into account when applying the calculation of the quadrupole invariants within the context of the IBM, as was pointed out by Dobaczewski et al. [104].

### A. Kumar method

The approach of Kumar makes use of the intrinsic quadrupole moment, which is:

$$Q_{s\mu}^i = \sqrt{\frac{16\pi}{5}} \int \rho_s r^2 Y_{2\mu} dV. \quad (5)$$

In this notation  $Q_{s\mu}^i$  is the  $\mu$ th component of the quadrupole moment of an equivalent ellipsoid of the nucleus, with charge density  $\rho_s$ . Furthermore, because of its reflection symmetry, for the quadrupole components of the ellipsoid it can be shown that [80, 85]:

$$\begin{aligned} Q_{s2}^i &= Q_{s,-2}^i, \\ Q_{s1}^i &= Q_{s,-1}^i = 0. \end{aligned} \quad (6)$$

The non vanishing components are written per definition as [80, 85]:

$$\begin{aligned} Q_{s0}^i &= Q_s^i \cos \gamma_s, \\ Q_{s2}^i &= Q_{s,-2}^i = \frac{Q_s^i}{\sqrt{2}} \sin \gamma_s. \end{aligned} \quad (7)$$

The invariant  $P_s^{(2)}$  of equation (3) is now rewritten by replacing the reduced matrix elements of the  $E2$  operators  $P_{2\mu}$  with the intrinsic quadrupole moments given in (5). This way the invariants for  $n = 2$  and 3 are expressed by  $Q_{s\mu}^i$  and  $\gamma_s$ , and, due to equation (7), they are expressed by  $Q_s^i$ . This way one finally gets the expressions [80]:

$$Q_s^i = \sqrt{\frac{16\pi}{5}} \sqrt{P_s^{(2)}}, \quad (8)$$

$$\cos 3\gamma_s = -\sqrt{\frac{7}{2}} \frac{P_s^{(3)}}{\left(P_s^{(2)}\right)^{\frac{3}{2}}}. \quad (9)$$

Although the intrinsic quadrupole moment  $Q_s^i$  in (8) already is an expression of the nuclear deformation, it is convenient to express the nuclear shape by the usual deformation parameters  $\beta$  and  $\gamma$ . Therefore a calculation of  $\beta$  defined by the ratio of the quadrupole moment over the monopole moment is useful:

$$\beta_{s\mu} = \frac{4\pi \int \rho_s r^2 Y_{2\mu} dV}{5 \int \rho_s r^2 dV} = \sqrt{\frac{\pi}{5}} \frac{Q_{s\mu}^i}{Z \langle s | r^2 | s \rangle}. \quad (10)$$

The normalization factor  $\frac{4\pi}{5}$  has been chosen so that the deformation parameter matches with  $\beta$  of Bohr and Mottelson [85]. Since the proportionality factors in (10) are independent of  $\mu$ , the tensor  $\beta_{s\mu}$  follows the same relations as  $Q_{s\mu}^i$  in equations (6) and (7) and thus it is sufficient to focus on the magnitude of the deformation  $\beta_s$  instead of  $\beta_{s\mu}$ . The remaining difficulty now is to calculate the monopole moment  $\langle r^2 \rangle$ . This can be done by calculating  $\langle r^2 \rangle$  for an equivalent ellipsoid of equal volume (or  $R_0^3$ ) with charge density obtained by uniformly distributing the charge  $Ze$  over the ellipsoid and where  $P_s^{(2)}$  and  $P_s^{(3)}$  are equal to those of the nucleus in the given state  $|s, M_s\rangle$ . Kumar [80] has shown that extracting the value of  $\beta$  under the above condition is equivalent to solving the cubic equation:

$$\delta_s^3 (g_s^3 - 2 \cos 3\gamma_s) + 3\delta_s^2 - 1 = 0, \quad (11)$$

with the relation between  $\delta_s$  and  $\beta_s$  expressed as

$$\delta_s = \beta_s / \sqrt{\frac{4\pi}{5}}, \quad (12)$$

and  $g_s = \frac{6ZR_0^2}{5Q_s^i}$ . It is important to mention that the values  $Q_s^i$  and  $\cos 3\gamma_s$  define the deformation characteristics associated with the given state  $s$ , the extraction of deformation parameters  $\beta$ ,  $\gamma$  imply a certain model assumption, which is very general though.

### B. Recent analyses methods: Cline-Flaum approach

In most of the recent papers it is more common to use a slightly different notation for the invariants  $P_s^{(2)}$  and  $P_s^{(3)}$ , which was initially introduced by D. Cline [81]. Besides the difference in notation there is a difference in prefactors, which can result in some confusion, when comparing both notations <sup>1</sup>.

Here, one starts from the knowledge that the expectation value of a tensor rank zero operator,  $[E2 \otimes E2]_0^{(0)}$ ,  $[[E2 \otimes E2]^{(2)} \otimes E2]_0^{(0)}$ , is independent of the reference frame. Evaluating the above tensor products within the principal axis frame, the quadrupole operator is described by two non-vanishing quadrupole operators, only.

<sup>1</sup> Kumar is deriving the invariants by making a transformation from a tensor product to a scalar product, when coupling  $E2$  matrix elements ( $P_2 \cdot P_2 = \sqrt{5} [P^{(2)} \otimes P^{(2)}]_0^{(0)}$ ) to produce the angular momentum zero coupling. In this section the invariants are derived by tensor couplings exclusively, resulting in a general difference in factors of  $\sqrt{5}$ , when comparing both methods.

One makes the choice of  $E2_0 = Q\cos\delta$ ,  $E2_{\pm 2} = Q\sin\delta\frac{1}{\sqrt{2}}$ ,  $E2_{\pm 1} = 0$ .

Analogous to (3) one now derives the result [81]:

$$\begin{aligned} \langle i | [E2 \otimes E2]_0^{(0)} | i \rangle &= \frac{1}{\sqrt{5}} \frac{1}{2I_i + 1} \sum_t |\langle i || E2 || t \rangle|^2 \\ &= \frac{1}{\sqrt{5}} \langle Q^2 \rangle. \end{aligned} \quad (13)$$

The matrix elements involved are now denoted by  $\langle i || E2 || t \rangle$  instead of  $M_{sr}$  as before. A comparison of both formulas shows indeed that  $\langle Q^2 \rangle = P_i^{(2)}$ , which in turn is equal to a summation of  $B(E2)$ -values, indicating the equivalence of both methods in evaluating the quadratic invariants. In the same way one obtains for the coupling of three operators analogous to invariant  $P_s^{(3)}$  of equation (4) [81, 94]:

$$\begin{aligned} &\langle i | \left[ [E2 \otimes E2]^{(2)} \otimes E2 \right]_0^{(0)} | i \rangle \\ &= \frac{(-1)^{2I_i}}{2I_i + 1} \sum_{t,u} \langle i || E2 || u \rangle \langle u || E2 || t \rangle \langle t || E2 || i \rangle \\ &\quad \times \left\{ \begin{array}{ccc} 2 & 2 & 2 \\ I_i & I_u & I_t \end{array} \right\}. \end{aligned} \quad (14)$$

Carrying out the recoupling when working in the principal axis frame, the expectation value of the cubic invariant becomes

$$\langle i | \left[ [E2 \otimes E2]^{(2)} \otimes E2 \right]_0^{(0)} | i \rangle = -\sqrt{\frac{2}{35}} \langle Q^3 \cos(3\delta) \rangle. \quad (15)$$

Here the deformation parameter expressing triaxiality is denoted by  $\delta$ . Keeping in mind that  $\langle Q^3 \rangle = (P_i^{(2)})^{\frac{3}{2}}$  one obtains exactly the same expressions using the Kumar convention as when using the notation of the present subsection to calculate the invariant  $P_i^{(3)}$  (or  $\langle i | [[E2 \times E2]_2^{(2)} \times E2] | i \rangle$  respectively) and, thus,  $\gamma_s$  equals  $\delta$ .

In most experimental papers, starting from reduced  $E2$  matrix elements ( $\langle || E2 || \rangle$ ) obtained using Coulomb excitation, the values of  $\langle Q^2 \rangle$  and  $\langle Q^3 \cos(3\delta) \rangle$ , can be extracted for each individual excited state. Having come this far, it is important to mention that the quadrupole invariants do play a role as extracted ‘‘observables’’, being constructed from measured reduced  $E2$  matrix elements, and as such express the nuclear deformation characteristics in a condensed way through the sums  $P_s^{(2)}$ ,  $P_s^{(3)}$  and this for a given nuclear state described by the quantum numbers  $s$  (Kumar notation), or  $i$  (Cline notation).

They are both useful and significant in presenting the way in which the nuclear excited states are ‘‘correlated’’ through a subset of collective degrees of freedom, expressed mostly using the Bohr-Mottelson  $\beta$ ,  $\gamma$  parameters. A problem, at present, is still the knowledge of too few data because of the difficulties to extract rather complete sets of reduced  $E2$  matrix elements using Coulomb

excitation [14–16]. Therefore, there is need for experiments that use higher-energy Coulomb excitation, which is one of the goals of HIE-ISOLDE project [105].

It is interesting though (see Kumar method) to transform the  $\langle Q^2 \rangle$  and  $\langle Q^3 \cos(3\delta) \rangle$  invariants into corresponding  $\langle \beta^2 \rangle$  and  $\langle \beta^3 \cos(3\gamma) \rangle$  values. An extensive study has been carried out by Srebrny *et al.* [94] describing deformed nuclei by a Nilsson ellipsoidal deformed potential [106–108], equating the experimental (or theoretical, as derived from our present LSSM calculations)  $P_s^{(2)}$ ,  $P_s^{(3)}$  invariants with the corresponding theoretical values. This results in the relations

$$Q^2 = \left( \frac{3}{4\pi} ZeR_0^2 \right)^2 (\beta^2 + \mathcal{O}(\beta^3)), \quad (16)$$

and

$$Q^3 \cos(3\delta) = \left( \frac{3}{4\pi} ZeR_0^2 \right)^3 (\beta^3 \cos(3\gamma) + \mathcal{O}(\beta^4)) \quad (17)$$

(whereas in Kumar’s approach, no such expansion is needed).

It can also be shown that within the context of Hartree-Fock-Bogoliubov microscopic calculations, only the lowest order contribution results, for both equation (16) and (17). In general, small differences in the extracted values of  $\beta$ ,  $\gamma$  may result depending on the precise definition of the collective variables (see e.g. [93]). The higher order terms of equations (16) and (17) can be found in the appendix of [94].

We note that in the treatments of Kumar and Cline [81, 94, 97], sums of products of  $E2$  matrix elements are defined for fluctuations in the invariants. This is important when addressing experimental data. Herein, we present detailed maps of all of the  $E2$  strength which, de facto, represent a very high resolution decomposition of the fluctuational content of the centroids.

### C. Deformation analysis: application to the harmonic oscillator

Before moving into a detailed discussion of the deformation properties for the light Cd nuclei, spanning the region in between mass number  $A = 98$  and  $A = 108$ , we have carried out a schematic analysis of the Kumar-Cline sum-rule method extracting the invariants when applied to a harmonic vibrator model. Consequently, we have an exact test of the sum-rule method when applied for vibrational nuclei in the evaluation of the value of  $\langle \beta^2 \rangle$  [3, 109].

Within the harmonic vibrator model with an homogeneous charge distribution, the resulting collective model electric operator, describing harmonic vibrational motion [85] with multipolarity  $\lambda$  is defined by:

$$\mathcal{M}(E\lambda) = \frac{3}{4\pi} Z e R^\lambda \hat{\alpha}_{\lambda\mu}, \quad (18)$$

with  $\hat{\alpha}_{\lambda\mu}$ , the collective coordinates describing the oscillatory behavior.

This results in the well-known variation of the mean-square charge radius, which can be derived as [109]:

$$\begin{aligned} \beta_N^2 &= \langle \alpha, N, JM | \sum_{\mu} \hat{\alpha}_{2\mu}^* \hat{\alpha}_{2\mu} | \alpha, N, JM \rangle, \\ &= \frac{\hbar\omega_2}{2C_2} (5 + 2N), \end{aligned} \quad (19)$$

with the phonon number  $N$ , spin  $J$  and spin projection  $M$ .

It can easily be shown in an example calculation, using the restricted framework of an ideal vibrator, where both states and transition strength of the phonons are known, that a simple application of sum rules to (19) results in the calculation of invariants for the ideal vibrator including the correct energy dependency as in (19).

We first consider the ground state  $0_1^+$ . Here, the sum in eq. (13) only contains the  $2_1^+$  state as intermediate state, with a result similar to  $\langle Q^2 \rangle = q_0^2 \frac{5\hbar\omega_2}{2C_2}$ , where  $q_0$  according to equation (16) is defined by  $q_0 = \frac{3}{4\pi} Z e R_0^2$ . This straightforwardly identifies the invariant analyses with the correct value by  $\langle \beta^2 \rangle$  for the ground-state vibrational mode. As a proof of concept the example of the sum rule calculation for the first phonon ( $N = 1$ ) state  $2_1^+$  will be shown too:

$$\langle 2_1^+ | \sum_{\mu} |\alpha_{2\mu}|^2 | 2_1^+ \rangle = \frac{1}{5} \sum_{J,f} (-1)^J |\langle 2_1^+ || \hat{\alpha}_2 || J_f \rangle|^2. \quad (20)$$

Let us remark that the right-hand side can also be written as  $\sum_{J,f} B(E2; 2_1^+ \rightarrow J_f)$ . In this case the sum of (20) runs over  $J_f = 4_1^+, 2_2^+, 0_2^+$  and  $0_1^+$  only. Thus, with respect to the normalized transition strength of the harmonic oscillator phonon levels to the first ( $2_1^+ \rightarrow 0_1^+$ ) phonon transition [85]:

$$\begin{aligned} \sum_{J_{N-1}} B(E2; N, J_n \rightarrow N-1, J_{N-1}) \\ = N \cdot B(E2; N=1 \rightarrow N=0), \end{aligned} \quad (21)$$

and taking  $B(E2; N=1 \rightarrow N=0) := 1$  the sum of (20) results into:

$$\left(1 + \frac{2}{5} + \frac{10}{5} + \frac{18}{5}\right) \frac{\hbar\omega_2}{2C_2} = 7 \frac{\hbar\omega_2}{2C_2}. \quad (22)$$

We recall, that the quadrupole moment of a pure harmonic oscillator is zero and thus in the sum of (20)  $\langle 2_1^+ || \hat{\alpha}_2 || 2_1^+ \rangle = 0$ . The outcome of (22) is fully consistent with the expected result from (19).

This example demonstrates the direct connection between the invariant  $P_s^{(2)}$ , the deformation parameter

$\beta_s = \sqrt{\langle \beta^2 \rangle}$  and the collective coordinates  $\alpha_{2\mu}$ . Although the mean square deformation  $\beta_s$ , derived from the invariants in the lab frame, and  $\beta$ , originally defined as a collective coordinate, are of the same physical quality, by construction they are not the same physical quantity.

## IV. DEFORMATION ANALYSIS

### A. Deformation correlated to neutron number

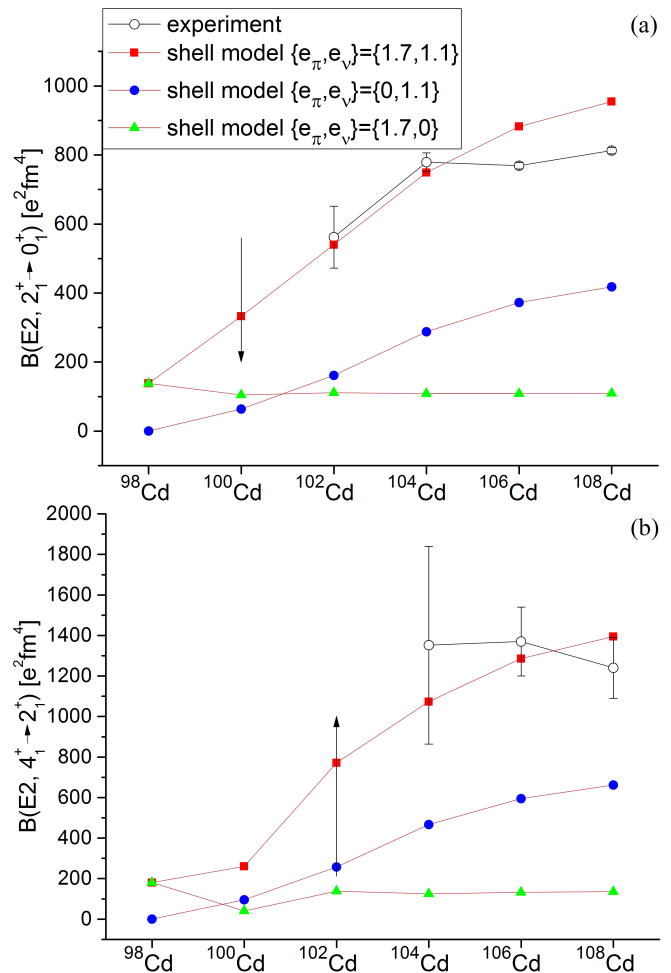


Figure 1. (a): The theoretical  $B(E2; 2_1^+ \rightarrow 0_1^+)$  values with red lines to guide the eye. We also present the separate contributions of protons (green triangles), neutrons (blue dots) and overall contribution to transition strength (red squares). The black circles present experimental results as well as data taken from [14] ( $^{100}\text{Cd}$ ), [13] ( $^{102,104}\text{Cd}$ ) and [16] ( $^{106,108}\text{Cd}$ ). (Color online).

(b): The theoretical  $B(E2; 4_1^+ \rightarrow 2_1^+)$  values compared to experimental results taken from [11] ( $^{102}\text{Cd}$ ), [13] ( $^{104}\text{Cd}$ ) and [15] ( $^{106,108}\text{Cd}$ ). (Color online).

A common tool for the analysis of collectivity in general is the  $E2$  transition strength of the first  $2_1^+$  state to the ground state. In the harmonic vibrator picture,

this transition is also considered to correspond to the one phonon transition and, because of its collective character, is expected to increase with the number of valence particles. In Figure 1 we present a comparison between the theoretical and experimental  $B(E2)$  values as well as the separate contributions corresponding with the proton and neutron part, in the shell-model calculations. The evolution of the theoretical  $B(E2)$  values follows a steady increase as a function of neutron number up to  $^{104}\text{Cd}$ . Here the experimental data indicate a leveling off whereas the theoretical  $B(E2)$  values are still increasing albeit less steep. The experimental data for the heavier Cd nuclei (beyond  $A = 108$ ) indicate a further increase, coming to a maximal value of  $1140 e^2 fm^4$  at neutron number 70 ( $A = 118$ ) before dropping again (see ref. [14]). On the other hand, these effective charges do not result in too large  $B(E2; 4_1^+ \rightarrow 2_1^+)$  values for the  $^{104-108}\text{Cd}$  nuclei as shown in Figure 1 (b). A slight reduction of the effective charges from  $(e_\pi, e_\nu) = (1.7e, 1.1e)$  to  $(1.6e, 1.0e)$  as in [14] would result in a better agreement with the  $B(E2; 2_1^+ \rightarrow 0_1^+)$  values for  $^{106,108}\text{Cd}$ , but the reproduction of the  $B(E2; 4_1^+ \rightarrow 2_1^+)$  data would deteriorate. Any small variation of the effective charges would result in small changes of the SM  $E2$  strengths used as an input for the deformation analysis performed in this work, thus preserving the overall validity of the deformation analysis results.

Considering the  $B(E2; 0_1^+ \rightarrow 2_1^+)$  transition as the only allowed transition starting from the  $0_1^+$  state, is of course an idealized picture in terms of exciting possible higher-lying  $2^+$  states for the Cd nuclei discussed here. On the other hand it is expected that the  $0_1^+ \rightarrow 2_1^+$  transition, on average, covers  $\sim 97\%$  of the summed  $E2$  transition strength  $\sum_f B(E2; 0_1^+ \rightarrow 2_f^+)$  [110, 111 see page 449] for medium and heavy mass nuclei. Because of the relation between the  $E2$  transition matrix elements and the quadrupole deformation, as discussed in Sections III A and III B, a behavior of the deformation describing the intrinsic properties of the  $0_1^+$  ground state, as a function of neutron number  $N$ , similar to Figure 1 (a) is expected (see Figure 2).

The present experimental status is such, that the  $2_1^+ \rightarrow 0_1^+$  and the  $2_2^+ \rightarrow 0_1^+$  transitions are the only transitions from a  $2^+$  state to the ground state with experimentally known  $B(E2)$  values in  $^{106}\text{Cd}$  and  $^{108}\text{Cd}$ . In  $^{100}\text{Cd}$ ,  $^{102}\text{Cd}$  and  $^{104}\text{Cd}$  only the  $B(E2)$  value of the  $2_1^+ \rightarrow 0_1^+$  transition is known, whereas for  $^{100}\text{Cd}$  only an upper limit is available. For  $^{98}\text{Cd}$ , no data about the  $2_1^+ \rightarrow 0_1^+$  transition strength is known. On the other hand, the present shell-model calculations include all  $E2$  transitions  $0_1^+ \rightarrow 2_f^+$  up to  $f = 50$  for  $^{100-106}\text{Cd}$  and up to  $f = 30$  for  $^{108}\text{Cd}$ <sup>2</sup>, which is a very large number of

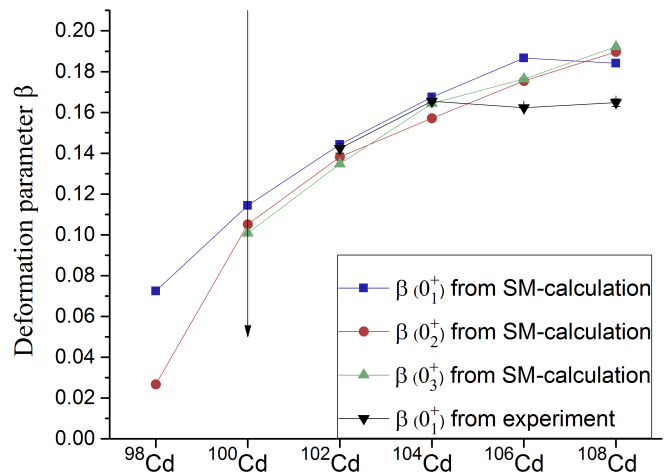


Figure 2. The calculated quadrupole deformation for the  $0_1^+$  (blue squares),  $0_2^+$  (red dots) and  $0_3^+$  (green triangles), compared with the experimental data ([14] ( $^{100}\text{Cd}$ ), [13] ( $^{102,104}\text{Cd}$ ) and [16] ( $^{106,108}\text{Cd}$ )) for the ground state only considering the  $2_1^+ \rightarrow 0_1^+$   $E2$  transition strength, to extract the value of  $\beta$ . (Color online).

states, and is expected to cover the full  $E2$  strength as compared to the experimentally known data.

In Figure 2 we present a comparison of the theoretical  $\beta$  values corresponding to the  $0_1^+$ ,  $0_2^+$  and  $0_3^+$  states, resulting from all calculated transitions and the experimental  $\beta$  value making use of the only known  $2_1^+ \rightarrow 0_1^+$   $E2$  transition [13, 14, 16] for the present Cd nuclei. (The shell-model based results shown here, are derived by the method as discussed in section III B). The fact that the  $\beta$  values extracted for the  $0_1^+$  ground states, making use of many  $E2$  transition matrix elements  $\langle 2_f^+ || E2 || 0_1^+ \rangle$ , resulting from the present shell-model calculations, and only one experimental transition matrix element, are very close for all nuclei considered, is a result of the dominant contribution of the  $0_1^+ \rightarrow 2_1^+$   $E2$  transition strength to the total sum, as argued before. The shell-model results exhibit the same behavior, as the sums  $\sum_{f=2}^M B(E2; 0_1^+ \rightarrow 2_f^+)$  over the non-yrast transitions cover only  $\sim 5\% - 6\%$  of the total sum. Figure 3 presents the sums of the transition strength for the three lowest  $0_{1,2,3}^+$  states with contributions from shell model  $2_f^+$  states as a function of energy of the  $2^+$  states for the nuclei  $^{100}\text{Cd}$  up to  $^{108}\text{Cd}$ . This figure which represents the  $E2$  strength function connected to the first three  $0^+$  states, at the same time exhibits the convergence of the sum in  $P_s^{(2)}$  and  $\langle Q^2 \rangle$  respectively (equations (3) and (13)) for the  $0_{1,2,3}^+$  states, for which transitions from states of higher energy ( $2_f^+$ ;  $f \gtrsim 30$ ) are only contributing in negligible amounts.

The way convergence is reached for the  $0_{2,3}^+$  levels exhibits a most interesting behavior with increasing mass. Whereas for the lighter isotopes ( $A = 100 - 104$ ) the curves are mainly characterized by a large number of in-

<sup>2</sup> The  $0_1^+ \rightarrow 2_f^+$  transitions of  $^{108}\text{Cd}$  have only been calculated up to  $f = 30$  to reduce the computation time, which is still sufficient to cover the full  $E2$  strength, as Figure 3 exhibits.

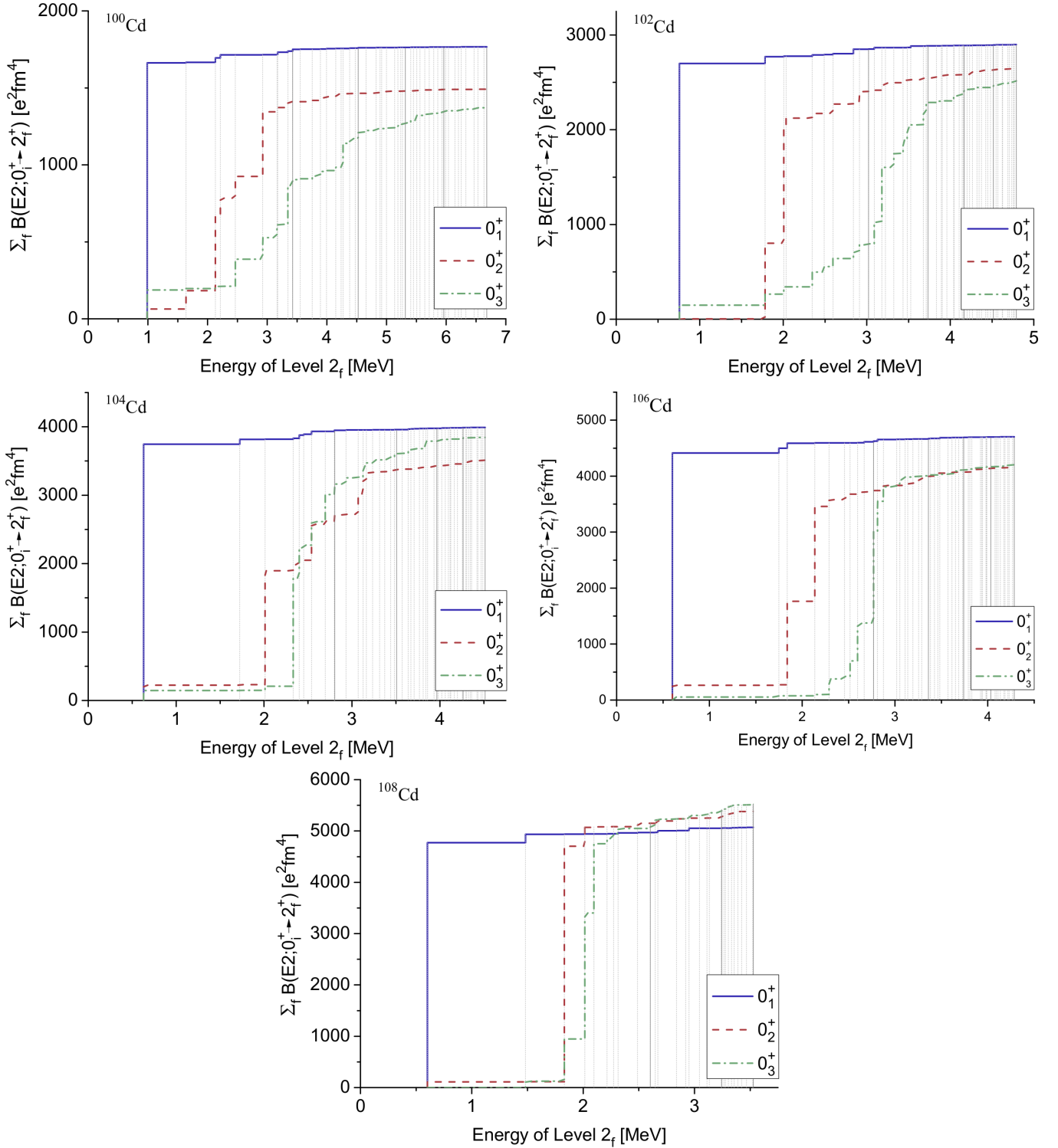


Figure 3. A graphical illustration of the contributions for each  $0_i^+$  state (with  $i = 1, 2, 3$ ) to the sums of equation (3) and (13) respectively, as a function of energy of the various  $2_f^+$  states (with  $f = 1, \dots, 50$  for  $^{100-106}\text{Cd}$  and  $f = 1, \dots, 30$  for  $^{108}\text{Cd}$ , respectively) on the horizontal axis. Vertical, dashed drop lines indicate the energies of the  $2_f^+$  states in each figure, with a solid drop line for every full set of ten  $2^+$  states. (Color online).

intermediate steps, an increasing concentration into just a few states shows up in approaching  $^{108}\text{Cd}$ . One observes a transition from a highly fragmented trend for the  $0_2^+$ , and even more so for the  $0_3^+$  state moving through the nuclei with, to a situation in  $^{108}\text{Cd}$ , with the  $0_2^+$  state exhibiting a similar character as the ground state. The total strength of each sum is in line with the extracted value of  $\beta$ , shown in Figure 2. What is thus interesting is the fact, that the strength functions of the  $0_3^+$  state and the lower  $0^+$  states are quite different even though the corresponding  $\beta$  values are very close to each other. In the latter case, one also notices that for the  $0_3^+$  state in  $^{108}\text{Cd}$ , the full strength is nearly reached within 3 steps, which is different from the lighter mass Cd nuclei. In those cases, where the full  $E2$  strength concentrates in a single state, the deformation parameter is associated to an intrinsic state. Mean field calculations of Prochniak et al. [78] point also in this direction.

At this place, we emphasize the importance of studying the strength functions in such detail, in order to understand the underlying structure of the states and band members. The  $E2$  strength functions, shown in Figure 3, are adding important information to the invariants calculated before using the Kumar-Cline method. Combining the information contained in Figures 2 and 3 and later also Figure 5, deep insight into the structure of in particular the ground state band, and to a lesser extent for the higher bands, is obtained.

The values of  $\beta$  are compared in Table I. The table displays, that the values of both deformation analysis methods differ only in the order of three places after the decimal point, which illustrates the excellent congruency of both approaches.

We notice, that no  $\beta$  value could be derived for the  $0_2^+$  state in  $^{98}\text{Cd}$  using the method of section III A in this LSSM model space. The nucleus  $^{98}\text{Cd}$  has a closed neutron shell and two proton holes within the  $1g_{9/2}$  and  $2p_{1/2}$  orbitals, which can couple to form excited states within the used model space. The  $^{98}\text{Cd}$   $E2$  transition scheme therefore consists mainly of an yrast band, characterized by seniority  $\nu = 2$  excitations, with the two proton holes placed in the  $1g_{9/2}$  orbital for each state of the band. The only other possible particle distribution producing positive parity states is, when the two proton holes are placed in the  $2p_{1/2}$  orbital, making up for a  $0_2^+$  state. Therefore besides the yrast-band the  $0_2^+ \rightarrow 2_1^+$  transition is the only possible  $E2$  transition. In comparison the  $0_1^+ \rightarrow 2_1^+$   $B(E2)$  value is approximately seven times stronger than the  $0_2^+ \rightarrow 2_1^+$   $B(E2)$  value. This leads to a "lack" in  $E2$  transition strength when calculating the  $P_s^{(2)}$  invariant for the  $s = 0_2^+$  state, relative to the  $P_s^{(3)}$  invariant, which involves, in addition, the quadrupole moment of the  $2_1^+$  intermediate state, with a three times stronger diagonal  $E2$  matrix element as compared to the  $0_2^+ \rightarrow 2_1^+$  transition  $E2$  matrix element. This results, according to equation (9), into a situation with  $P_s^{(3)}/(P_s^{(2)})^{\frac{3}{2}} > 1$  and, consequently,  $\gamma$  cannot be

calculated for the  $0_2^+$  which, in turn, is necessary for the derivation of  $\beta$ .

Using the concept that most nuclei exhibit some softness and, consequently, exhibit a tendency for deformation (be it static as for strongly deformed nuclei, or, in a dynamic way for soft nuclei in transitional regions and near to closed shells), any excited state is prone to be described using collective modes of motion (rotation, shape oscillations), implying that a nuclear shape is not a net "observable". Although the magnitude of the overall nuclear deformation  $\beta$  remains a well defined variable, the uncertainty in the nuclear shape  $\gamma$  (which can be quantified by calculating the variance, defined as  $\sigma(\langle Q^3 \rangle) \equiv \sqrt{\langle Q^6 \rangle - (\langle Q^3 \rangle)^2}$  (see also references [81, 94, 97])) is in general increasing with the increasing nuclear spin. Thus we do not consider  $\gamma$  values of other states than  $0_1^+$ , though they could in principle be calculated from the shell-model results. In Figure 4 the deformation parameter  $\gamma$  is shown for the ground state as a function of increasing mass number  $A(N)$ . Together with the information of Figure 2, one notices that  $\gamma$  is increasing with  $N$ , starting at a slightly prolate deformation in  $^{98}\text{Cd}$  of  $\gamma = 7.8^\circ$ . In  $^{108}\text{Cd}$  the  $\gamma$  value reaches a value  $17.5^\circ$  and thus is approaching the maximal triaxiality value of  $30^\circ$ , a value that separates the regions of prolate and oblate deformation. Therefore the overall shape of the ground states is to be considered as prolate with a growing triaxiality as the number of valence neutrons increases when starting to fill the  $N = 50-82$  shell. This result may support the picture of a  $\gamma$  soft structure in the light Cd isotopes, opposite to the traditional, vibrational picture.

Besides LSSM calculations, only few studies in the context of (beyond) mean-field studies have been performed. For the Cd nuclei mean-field calculations have been carried out by Prochniak et.al. [78] and Rodriguez and Egido [79]. In particular, in reference [78], total energy surfaces have been calculated for the  $^{106-116}\text{Cd}$  nuclei. In the mass span of  $A = 106$  to  $A = 108$ , a slight prolate minimum appears at a value of  $\beta \sim 0.15-0.2$ , a value quite close to the results of our shell-model based deformation analysis. The correspondence becomes even more pronounced when comparing the spectroscopic quadrupole moments derived from the mean-field results of ref. [78] for the  $2_{1,2,3}^+$  states. The resulting negative values for the  $2_{1,3}^+$  and a positive value for the  $2_2^+$  state, as well as the magnitudes are comparable to our SM results. This shows that both descriptions are very much consistent.

## B. Deformation correlated to spin

We have also studied the deformation for various excited states and the way this indicates the presence of correlations with the nuclear spin as one moves up in excitation energy. This study has been carried out by examining the deformation corresponding to the shell-model wave functions as a function of spin, up to  $J = 8$ ,



nucleus	$\beta$ value for $0_1^+$		$\beta$ value for $0_2^+$		$\beta$ value for $0_3^+$	
	sect. III A	sect. III B <sup>a</sup>	sect. III A	sect. III B <sup>a</sup>	sect. III A	sect. III B <sup>a</sup>
<sup>98</sup> Cd	0.0723	0.0725	-	0.0267	-	-
<sup>100</sup> Cd	0.1138	0.1144	0.1047	0.1051	0.1004	0.1008
<sup>102</sup> Cd	0.1435	0.1446	0.1371	0.1381	0.1338	0.1347
<sup>104</sup> Cd	0.1657	0.1675	0.1557	0.1571	0.1628	0.1644
<sup>106</sup> Cd	0.1842	0.1866	0.1734	0.1754	0.1744	0.1764
<sup>108</sup> Cd	0.1818	0.1841	0.1872	0.1890	0.1895	0.1922

Table I. Comparison of  $\beta$  values derived from the methods of section III A and III B (see Figure 2). <sup>a</sup>We emphasize, that the results of section III B are the root-mean square values, i. e.  $\sqrt{\langle 0_i^+ | \beta^2 | 0_i^+ \rangle}$ .

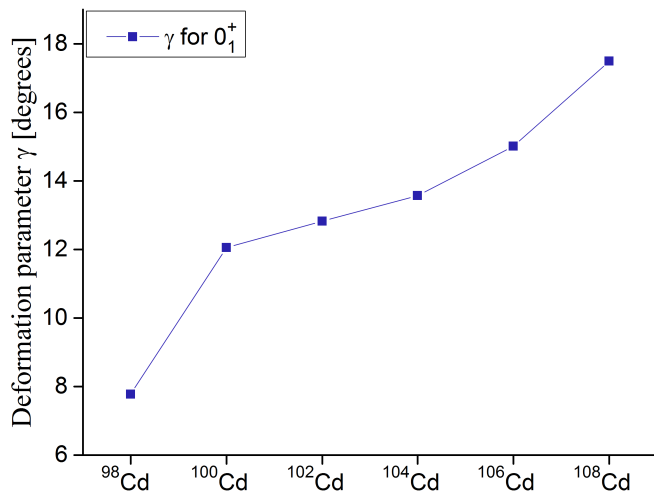


Figure 4. The deformation parameter  $\gamma$  extracted for the different isotopes. (Color online).

thereby following the deformation through a set of states defined as a band, as derived from the shell-model. In Figure 5 such bands are shown for the nuclei <sup>100</sup>Cd up to <sup>108</sup>Cd, in all of which two bands could be identified. The way in which we define a given band is by studying where the strongest  $E2$  matrix elements appear, when moving up in excitation energy through the spin sequences of  $0^+$ ,  $2^+$ ,  $4^+$ ,  $6^+$  in steps of  $\Delta J = 2$  until the  $8^+$  states and starting at the  $0_1^+$  and  $0_2^+$  states, respectively. In the resulting band structure any possible deexcitation from any state of band 1 will most probably end in the ground state, whereas a deexcitation of any state of band 2 will most probably end up into  $0_2^+$  respectively ( $M1$  branches are excluded in this study). A detailed study of the spectroscopy of these Cd nuclei, including comparisons with the large set of experimental data available at present, on issues such as low-lying states, high-spin bands, detailed spectroscopic information on moments, will form the content of a forthcoming paper.

In Figure 5 results of the deformation parameter  $\beta$  are given for the members of bands 1 and 2 in <sup>100</sup>Cd - <sup>108</sup>Cd, as well as for the  $8_1^+$  and  $8_2^+$  states in <sup>108</sup>Cd. When analyzing the evolution of state deformation for band 1 of all

considered nuclei and comparing the deformation curves, a number of characteristic similarities in all the nuclei show up. Starting at the  $0_1^+$  level one notices that the deformation is slightly increasing when moving into the  $2^+$  level for each band. Then a decrease in deformation follows, when going from  $2^+$  to  $4^+$ , except for <sup>104</sup>Cd where one again observes a slight increase but weaker than before, even close to stagnation in deformation as compared to the former step. For higher spins, beyond  $4^+$  and from <sup>102</sup>Cd on, the decrease in deformation is enhanced until  $J^\pi = 8^+$ . Such a trend could be explained qualitatively by looking at the sources of  $E2$  transition strength not only but especially between the band members. As the number of valence neutron pairs increases, going from <sup>100</sup>Cd to <sup>108</sup>Cd, the contribution of configurations allowing seniority changing transitions also increases, which affects stronger transitions between the low spin states, i.e.  $0^+$ ,  $2^+$ ,  $4^+$ . In addition, even small admixtures of neutron stretched  $E2$  transitions ( $\Delta j = \Delta l = 2$ ), which in this model space are only of the type  $2d_{5/2} \longleftrightarrow 3s_{1/2}$  will increase the total  $E2$  strength and consequently the deformation  $\beta$ . As the lowest seniority configurations, for which one or two neutrons are in the  $3s_{1/2}$  orbital, and the other valence neutrons occupying the rest of the neutron orbitals, can only produce low spins (for example the coupling of  $2d_{5/2} \otimes 3s_{1/2}$  is limited to  $2^+$  and  $3^+$ , while the members of the  $1g_{7/2} \otimes 3s_{1/2}$  multiplet have spins  $3^+$  and  $4^+$ ), this additional  $E2$  strength is concentrated between the low spin states up to  $4^+$ .

Generally, band 2 exhibits characteristics similar to the behavior of band 1, where an increase in deformation is observed in the step  $J = 0 \rightarrow J = 2$ , except for <sup>100</sup>Cd. The nuclei <sup>104</sup>Cd, <sup>106</sup>Cd and <sup>108</sup>Cd are very good examples for this behavior with  $\Delta\beta \approx 0.01$  in the step when going from  $0_2^+$  to the  $2^+$  member of band 2. For the steps from  $2^+$  until  $8^+$ , similar to the case with band 1, an overall decrease in deformation is observed. In <sup>102</sup>Cd for  $J = 4 \rightarrow J = 6$  the decrease in deformation escalates, resulting in a less smooth deformation curve compared to band 1. With these similarities, it can be stated that the maximum in deformation is located at the  $2^+$  band member (except for band 1 in <sup>104</sup>Cd where the  $4^+$  is at the maximum value, and band 2 in <sup>100</sup>Cd where deformation is decreasing from  $0_2^+$  onwards).

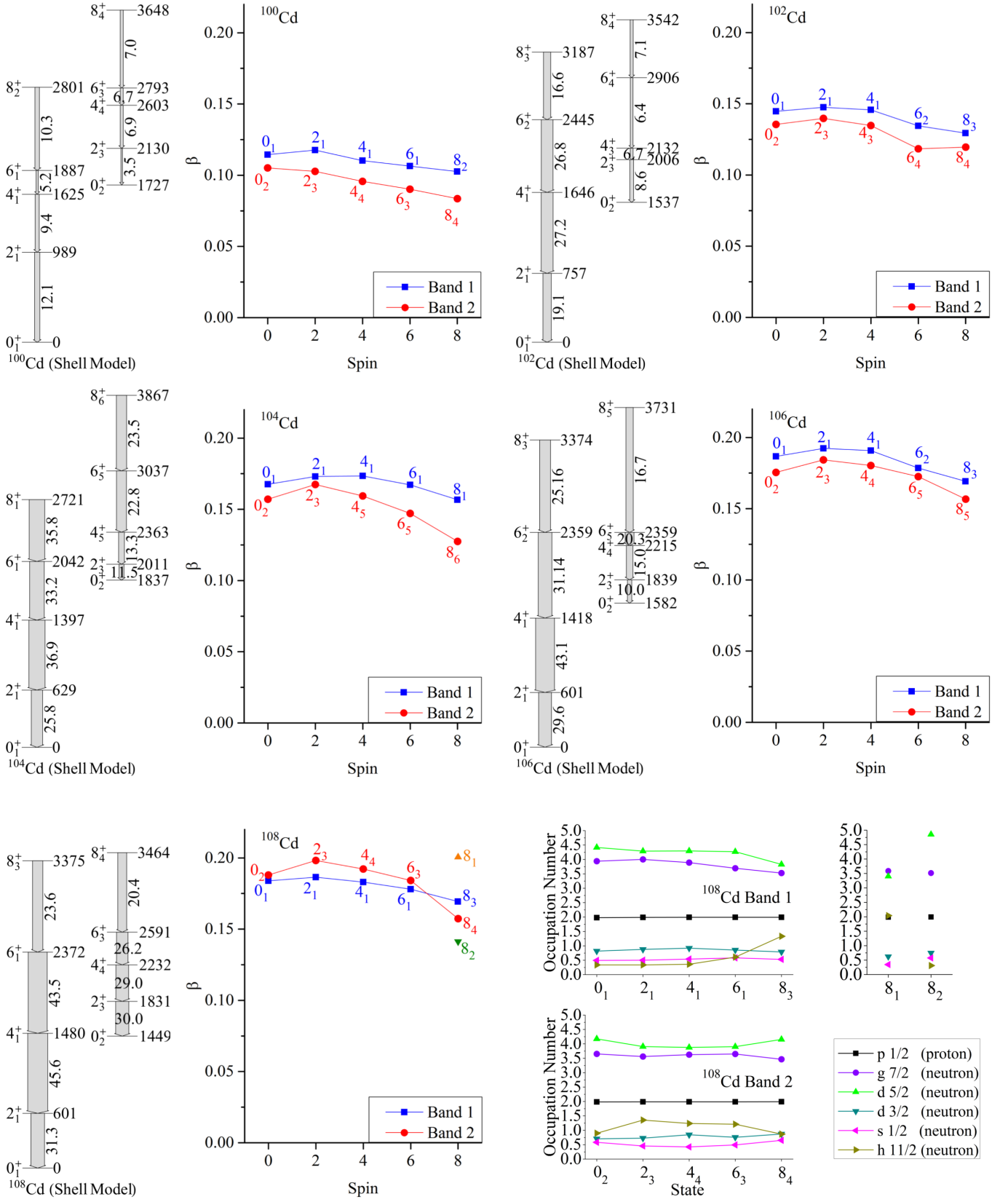


Figure 5. Partial level schemes with energies in [keV] and transition strengths in [W.u.] grouped in band structures for  $^{100}\text{Cd}$  -  $^{108}\text{Cd}$ . On the right-hand side of each figure the  $\beta$  deformation as a function of increasing spin is displayed, whereas blue squares denote values for members of band 1, connected to the ground state and red dots denote values for members of band 2 ending up in the  $0_2^+$  state. In the bottom right part of the figure, the specific orbital occupation of the two bands in  $^{108}\text{Cd}$  is presented as a function of increasing spin. The deformation and orbital occupation of the  $8_1^+$  and  $8_2^+$  state in  $^{108}\text{Cd}$  are given as additional examples. (Color online).

Besides these similarities in the deformation characteristics of the examined nuclei, the overall deformation strength of band 2 in  $^{108}\text{Cd}$  exceeds the deformation of band 1, which exhibits a change in the nuclear structure, as this behavior is not present in the lighter nuclei. These changes in deformation characteristics may well be associated with the particular occupation numbers of the various orbitals in  $^{108}\text{Cd}$ .

At the bottom right part of Figure 5 the related orbital occupation numbers of band 1 and 2 of  $^{108}\text{Cd}$  are displayed. The orbital occupation numbers shown in Figure 5 have been calculated using the shell-model wave functions resulting from the present calculations. A detailed examination of the orbital filling shown in Figure 5 indicates, that the increasing occupation of the  $1h_{11/2}$  orbital originates mainly from a depletion of the  $2d_{5/2}$  orbital, and this for all spin values in the two bands. This is especially obvious, when going from the  $6_1^+$  to the  $8_3^+$  state in band 1. The occupation number of the  $2d_{5/2}$  is lowered by an amount of  $\Delta \approx -0.5$  and the occupation of the  $1h_{11/2}$  is raised by  $\Delta \approx 0.7$ . It can nearly be considered as a neutron moving from the  $2d_{5/2}$  to the  $1h_{11/2}$  orbital. Also minor contributions from other orbitals can be observed, e.g. resulting from excitations from the  $1g_{7/2}$ ,  $2d_{3/2}$  and  $3s_{1/2}$  orbitals to the neutron  $1h_{11/2}$  orbital.

When comparing the deformation curve of band 2 in  $^{108}\text{Cd}$  to the curve showing the occupation of the  $1h_{11/2}$  orbital in band 2, it is obvious that neutrons in the  $1h_{11/2}$  orbital are affecting the deformation. In those states, where the  $1h_{11/2}$  orbital occupation is increasing, the corresponding deformation of band 2 is enhanced. Although both curves show a similar shape, the relation between the deformation of band 2 and the occupation of the  $1h_{11/2}$  orbital is not directly proportional.

In band 1 of  $^{108}\text{Cd}$  the deformation strength is also effected by the filling of the  $1h_{11/2}$  orbital. This is not as obvious from the shape of the deformation curve, but the influence caused by the  $1h_{11/2}$  can be illustrated by comparing the decrease in deformation over the steps from  $4^+$  to  $8^+$  for the various nuclei presented. In  $^{100}\text{Cd}$ ,  $^{102}\text{Cd}$ ,  $^{104}\text{Cd}$  and  $^{106}\text{Cd}$  these drops in deformation amount to  $\Delta\beta(4^+ \rightarrow 8^+) \equiv \beta(4^+) - \beta(8^+) = 0.008, 0.016, 0.017$  and  $0.022$  respectively, thus exhibiting an increasing drop of the deformation. In the case of  $^{108}\text{Cd}$  on the other hand, this trend is hindered by the drop amount of  $\Delta\beta(4^+ \rightarrow 8^+) = 0.014$ .

Two further examples which confirm the importance of the  $1h_{11/2}$  orbital on the deformation for the high-spin  $8_1^+$  and  $8_2^+$  states, resulting from the shell-model calculations, are highlighted. The calculated excitation energies are 2755 keV and 3136 keV, respectively. The  $8_1^+$  state exhibits the largest deformation  $\beta = 0.20$  found in the examined states in  $^{98}\text{Cd}$  -  $^{108}\text{Cd}$ , whereas the  $8_2^+$  shows the lowest deformation of the examined states in  $^{108}\text{Cd}$  with  $\beta = 0.14$ . Comparing the orbital occupation numbers of these two states, one notices that the major differences result from the filling of the  $2d_{5/2}$  and the  $1h_{11/2}$  orbitals. In the  $8_1^+$  state the  $2d_{5/2}$  and  $1h_{11/2}$  orbitals are filled with

$\approx 3.4$  and  $\approx 2$  neutrons respectively, whereas in the  $8_2^+$  state the  $2d_{5/2}$  orbital contains  $\approx 4.8$  and the  $1h_{11/2}$  orbital  $\approx 0.3$  neutrons. This looks like a neutron  $2p - 2h$  excitation from the  $2d_{5/2}$  into the  $1h_{11/2}$  orbital, causing a clear difference in the resulting deformation when comparing the  $\beta$  values for the  $8_1^+$  state with the  $8_2^+$  state (notice the  $\nu h_{11/2}$  occupation number in Figure 5). It turns out that the shell-model  $8_2^+$  state exhibits a proton  $1g_{9/2}^{-2}$  character, whereas experimental studies of  $^{108}\text{Cd}$  show that the  $8_1^+$  state at 3111 keV is of proton character and the  $8_3^+$  state at 3862 keV is of neutron  $1h_{11/2}^2$  character [112]. In the same study it was found, that the  $1h_{11/2}$  orbital is playing a dominant role in the low and high spin structure of  $^{108}\text{Cd}$  with a shape driving effect.

## V. SUMMARY AND CONCLUSIONS

In the present paper, we have studied how to extract the changing quadrupole collectivity and its associated deformation using input from large-scale shell-model calculations (LSSM) of the light  $^{98-108}\text{Cd}$  nuclei. The effective interaction used in the present study succeeds rather well in describing the overall variations in the excitation energy of the low-spin states in the Cd nuclei (spanning the  $A = 98$  to  $A = 108$  region) [89], in particular the excitation energy for the  $2_1^+$  state, as well as the increasing trend in the  $B(E2; 2_1^+ \rightarrow 0_1^+)$  value. This is an indication of a well-balanced description in which both the monopole and quadrupole components of the force and the induced polarization for the protons and neutrons, as obtained here, form a well-balanced system.

We emphasize that large-scale shell-model calculations (LSSM) can and have been carried out within a symmetry-dictated truncation basis (whenever the single-particle states spanning the model space are prone to such truncations). More in particular, both the quasi-SU(3) [113, 114] as well as the pseudo-SU(3) [115, 116] variants of Elliott's SU(3) model [117, 118] provide such options. Applications have been carried out in this spirit for the  $N = 20, 40, 48, \dots$  and even heavier nuclei [5, 88, 119, 120]

The sdg (excluding the  $1h_{11/2}$  unnatural parity orbital) neutron shell is apt to such an approach. Such calculations may allow to obtain a deeper insight in the results from a LSSM study about how quadrupole collectivity is developing in the Cd isotopes, and this as a function of increasing neutron number.

We have been able, using the calculated  $E2$  reduced matrix elements starting from the shell-model wave functions, defined within the laboratory framework, to derive both the quadratic and cubic quadrupole invariants. Using the fact that these invariants contain information about the nuclear deformation, defined within a frame of the principal axis of the nucleus, we are able to quantify the changing quadrupole deformation parameters  $\beta$  and  $\gamma$  in an almost model-independent way.

The first part (section III) presented a rather detailed comparison of two methods that have been (and are) used to derive the intrinsic deformation characteristics, extracted from the quadrupole invariants. Here, the aim was to discuss the slight and often subtle differences between both approaches that lead to apparent slightly different expressions in the major papers and how, precisely, the intrinsic shape parametrization is extracted. This method is called in most papers "model independent", an issue which we discuss in some detail pointing out how, even though very general, generic features related to quadrupole deformed and intrinsic shape can be described and parametrized.

The comparison between the calculated  $B(E2; 2_1^+ \rightarrow 0_1^+)$  reduced transition probabilities and the known data for the Cd nuclei with  $50 \leq N \leq 60$ , showed that the LSSM reproduces well the collectivity. For the presented variation of the extracted deformation, characterized by  $\beta$  starting at  $^{98}\text{Cd}$ , one observes an expected, rapid increase, followed by saturation when reaching the  $^{106,108}\text{Cd}$  isotopes. Moreover, inspecting the  $\beta$  value extracted from the set of levels that are strongly connected to the  $0_1^+$  and  $0_2^+$  "band-head levels", through a sequence of particularly strong  $E2$  transition matrix elements, one observes two separate bands characterized by  $\beta$  values, that are strongly "correlated" as a function of increasing angular momentum up to spin  $8^+$  states. We also notice that within each of those bands, there is not a particular increase in the value of  $\beta$  as a function of increasing angular momentum, which would be expected, even for close to harmonic vibrational collective quadrupole motion, at least up to mass number  $A = 102$ . In the  $^{106,108}\text{Cd}$  nuclei, an initial slight increase is observed, followed by a decrease with increasing spin up to  $8^+$ . In  $^{108}\text{Cd}$ , a specific upslope in  $\beta$  shows up and it turns out that this effect can be associated with a redistribution of neutrons from the  $2d_{5/2}$  into the  $1h_{11/2}$  shell-model orbital (the latter orbital is characterized by a larger value of  $\langle |r^2| \rangle$  when using harmonic oscillator radial wave functions).

An interesting conclusion from the present LSSM calculations is the observation that the  $0_2^+$  and  $0_3^+$  as well as associated band members exhibit similar  $\beta$  values as the ones obtained for the  $0_1^+$  ground state. Different values would be expected from a purely collective vibrational model approach to describe the quadrupole collec-

tive characteristics of these light Cd nuclei. We do not exclude that part of this may well be due to the fact that the model space does not contain proton  $np - nh$  excitations across the  $Z = 50$  closed shell (even though such correlations are implicitly included by the use of proton as well as neutron effective charges). Consequently, explicit breaking of the proton  $Z = 50$  shell is not incorporated in a direct way (we refer to [66] for an extensive study of so-called intruder states as well as to a recent focus issue on shape coexistence [121]). This is an issue to be explored in more detail, using more specific shell-model truncation schemes and model spaces which include  $np - nh$  proton excitation to study Cd isotopes.

The present paper has concentrated on the deformation characteristics for the lighter Cd nuclei. It is to be understood that a more detailed comparison of the extensive spectroscopic information for the set of Cd isotopes with mass number ranging from  $A = 98$  up to  $A = 108$  will follow. Thereby, both the low-spin energy spectra as well as the high-spin structure is studied. Moreover, when known, electromagnetic moments (electric quadrupole and magnetic dipole moments) will be compared with the present LSSM calculations as carried out at present.

We note that shortly before the submission of this work, new experimental results on  $B(E2)$  values and  $g$ -factors have become available (see [122]) but have not been addressed in our current paper. The reasons are (i) the fact that the  $B(E2)$  values in table III of [122] are inconsistent with previously published  $^{106}\text{Cd}$  values, and, (ii) these  $B(E2)$  values are inconsistent with the Cd systematics for the light Cd isotopes.

## ACKNOWLEDGMENTS

Financial support from the Interuniversity Attraction Poles Program of the Belgian State-Federal Office for Scientific and Cultural Affairs (IAP Grant P7/12) is acknowledged. We thank N. A. Smirnova for providing the effective shell-model interaction as well as intensive discussions in preparing the final version of this paper. We are grateful to J. L. Wood for extensive discussions during the course of this work, as well as for careful reading of the manuscript.

- 
- [1] A. Bohr, B. Mottelson, and D. Pines, Phys. Rev. **110**, 936 (1958).
  - [2] P. Ring and P. Schuck, *The Nuclear Many-Body problem* (Springer, Berlin-Heidelberg, 1980).
  - [3] D. J. Rowe and J. L. Wood, *Fundamentals of Nuclear Models; Foundational Models* (World Scientific Publishing, 2010).
  - [4] E. Caurier and F. Nowacki, Act. Phys. Pol. B **30**, 705 (1999).
  - [5] E. Caurier, G. Martinez-Pinedo, F. Nowacki, A. Poves, and A. P. Zuker, Rev. Mod. Phys. **77**, 427 (2005).
  - [6] M. Górska, R. Schubart, H. Grawe, J. B. Fitzgerald, D. B. Fossan, J. Heese, K. H. Maier, M. Rejmund, K. Spohr, and T. Rzaca-Urban, Z. Phys. A **350**, 181 (1994).
  - [7] M. Górska, M. Lipoglavšek, H. Grawe, J. Nyberg, A. Atac., A. Axelsson, R. Bark, J. Blomqvist, J. Ced-erkäll, B. Cedervall, et al., Phys. Rev. Lett. **79**, 2415 (1997).
  - [8] A. Blazhev, M. Górska, H. Grawe, J. Nyberg, M. Palacz,

- E. Caurier, O. Dorvaux, A. Gadea, F. Nowacki, C. Andreoiu, et al., *Phys. Rev. C* **69**, 064304 (2004).
- [9] A. Blazhev, N. Braun, H. Grawe, P. Boutachkov, B. S. Nara Singh, T. Brock, Z. Liu, R. Wadsworth, M. Górska, J. Jolie, et al., *J. Phys. Conf. Series G* **205**, 012035 (2010).
- [10] R. M. Clark, J. N. Wilson, D. Appelbe, M. P. Carpenter, C. J. Chiara, M. Cromaz, M. A. Deleplanque, M. Devlin, R. M. Diamond, P. Fallon, et al., *Phys. Rev. C* **61**, 044311 (2000).
- [11] K. P. Lieb, D. Kast, A. Jungclaus, I. P. Johnstone, G. de Angelis, C. Fahlander, M. de Poli, P. G. Bizzeti, A. Dewald, R. Peusquens, et al., *Phys. Rev. C* **63**, 054304 (2001).
- [12] N. Boelaert, N. Smirnova, K. L. G. Heyde, and J. Jolie, *Phys. Rev. C* **75**, 014316 (2007).
- [13] N. Boelaert, A. Dewald, C. Fransen, J. Jolie, A. Linne-mann, B. Melon, O. Möller, N. Smirnova, and K. L. G. Heyde, *Phys. Rev. C* **75**, 054311 (2007).
- [14] A. Ekström, J. Cederkäll, D. D. DiJulio, C. Fahlander, M. Hjorth-Jensen, A. Blazhev, B. Bruyneel, P. A. Butler, T. Davinson, J. Eberth, et al., *Phys. Rev. C* **80**, 054302 (2009).
- [15] W. T. Milner, F. K. McGowan, P. H. Stelson, R. L. Robinson, and R. O. Sayer, *Nucl. Phys. A* **129**, 687 (1969).
- [16] M. T. Esat, D. C. Kean, and R. H. Spear, *Nucl. Phys. A* **274**, 237 (1976).
- [17] G. de Angelis, C. Fahlander, D. Vretenar, S. Brant, A. Gadea, A. Algora, Y. Li, Q. Pan, E. Farnea, D. Bazzacco, et al., *Phys. Rev. C* **60**, 014313 (1999).
- [18] G. A. Müller, A. Jungclaus, O. Yordanov, E. Galindo, M. Hausmann, D. Kast, K. P. Lieb, S. Brant, V. Krstić, D. Vretenar, et al., *Phys. Rev. C* **64**, 014305 (2001).
- [19] S. F. Ashley, P. H. Regan, K. Andgren, E. A. McCutchan, N. V. Zamfir, L. Amon, R. B. Cakirli, R. F. Casten, R. M. Clark, W. Gelletly, et al., *Phys. Rev. C* **76**, 064302 (2007).
- [20] P. Datta, S. Chattopadhyay, S. Bhattacharya, T. K. Ghosh, A. Goswami, S. Pal, M. S. Sarkar, H. C. Jain, P. K. Joshi, R. K. Bhowmik, et al., *Phys. Rev. C* **71**, 041305 (2005).
- [21] P. E. Garrett, J. Bangay, A. Diaz Varela, G. C. Ball, D. S. Cross, G. A. Demand, P. Finlay, A. B. Garnsworthy, K. L. Green, G. Hackman, et al., *Phys. Rev. C* **86**, 044304 (2012).
- [22] D. Kusnezov, A. Bruder, V. Ionescu, J. Kern, M. Rast, K. L. G. Heyde, P. Van Isacker, J. Moreau, M. Waroquier, and R. A. Meyer, *Helv. Phys. Acta.* **60**, 456 (1987).
- [23] P. E. Garrett, K. L. Green, H. Lehmann, J. Jolie, C. A. McGrath, M. Yeh, and S. W. Yates, *Phys. Rev. C* **75**, 054310 (2007).
- [24] K. L. Green, P. E. Garrett, R. A. E. Austin, G. C. Ball, D. S. Bandyopadhyay, S. Colosimo, D. Cross, G. A. Demand, G. F. Grinyer, G. Hackman, et al., *Phys. Rev. C* **80**, 032502 (2009).
- [25] J. Kumpulainen, R. Julin, J. Kantele, A. Passoja, W. H. Trzaska, E. Verho, J. Väärämäki, D. Cutoiu, and M. Ivascu, *Phys. Rev. C* **45**, 640 (1992).
- [26] P. E. Garrett, K. L. Green, and J. L. Wood, *Phys. Rev. C* **78**, 044307 (2008).
- [27] D. Bandyopadhyay, S. R. Leshner, C. Fransen, N. Boukharouba, P. E. Garrett, K. L. Green, M. T. McEllistrem, and S. W. Yates, *Phys. Rev. C* **76**, 054308 (2007).
- [28] K. Schreckenbach, A. Mheemeed, G. Barreau, T. von Egidy, H. R. Faust, H. G. Börner, R. Brissot, M. L. Stelts, K. L. G. Heyde, P. Van Isacker, et al., *Phys. Lett. B* **110**, 364 (1982).
- [29] A. Mheemeed, K. Schreckenbach, G. Barreau, H. R. Faust, H. G. Börner, R. Brissot, P. Hungerford, H. H. Schmidt, H. J. Scheerer, T. Von Egidy, et al., *Nucl. Phys. A* **412**, 113 (1984).
- [30] S. Juutinen, P. Jones, A. Lampinen, G. Lhersonneau, E. Mäkelä, M. Piiparinen, A. Savelius, and S. Törmänen, *Phys. Lett. B* **386**, 80 (1996).
- [31] H. Mach, M. Moszyński, R. F. Casten, R. L. Gill, D. S. Brenner, J. A. Winger, W. Krips, C. Wesselborg, M. Büscher, F. K. Wahn, et al., *Phys. Rev. Lett.* **63**, 143 (1989).
- [32] Y. Wang, P. Dendooven, J. Huikari, A. Jokinen, V. S. Kolhinen, G. Lhersonneau, A. Nieminen, S. Nummela, H. Penttilä, K. Peräjärvi, et al., *Phys. Rev. C* **64**, 054315 (2001).
- [33] M. Kadi, N. Warr, P. E. Garrett, J. Jolie, and S. W. Yates, *Phys. Rev. C* **68**, 031306(R) (2003).
- [34] J. C. Batchelder, J. L. Wood, P. E. Garrett, K. L. Green, K. P. Rykaczewski, J. C. Bilheux, C. R. Bingham, H. K. Carter, D. Fong, R. Grzywacz, et al., *Phys. Rev. C* **80**, 054318 (2009).
- [35] A. Aprahamian, D. S. Brenner, R. F. Casten, R. L. Gill, A. Piotrowski, and K. L. G. Heyde, *Phys. Lett. B* **140**, 22 (1984).
- [36] Y. Wang, S. Rinta-Antila, P. Dendooven, J. Huikari, A. Jokinen, V. S. Kolhinen, G. Lhersonneau, A. Nieminen, S. Nummela, H. Penttilä, et al., *Phys. Rev. C* **67**, 064303 (2003).
- [37] Y. X. Luo, J. O. Rasmussen, C. S. Nelson, J. H. Hamilton, A. V. Ramayya, J. K. Hwang, S. H. Liu, C. Goodin, N. J. Stone, S. J. Zhu, et al., *Nucl. Phys. A* **874**, 32 (2012).
- [38] J. C. Batchelder, N. T. Brewer, R. E. Goans, R. Grzywacz, B. O. Griffith, C. Jost, A. Korgul, S. H. Liu, S. V. Paulauskas, E. H. Spejewski, et al., *Phys. Rev. C* **86**, 064311 (2012).
- [39] T. Kautzsch, W. B. Walters, V. N. Fedoseyev, Y. Jading, A. Jokinen, I. Klöckl, K.-L. Kratz, V. I. Mishin, H. L. Ravn, P. Van Duppen, et al., *Phys. Rev. C* **54**, R2811 (1996).
- [40] S. Ilieva, M. Thürauf, T. Kröll, R. Krücken, T. Behrens, V. Bildstein, A. Blazhev, S. Bönig, P. A. Butler, J. Cederkäll, et al., *Phys. Rev. C* **89**, 014313 (2014).
- [41] J. C. Batchelder, N. T. Brewer, C. J. Gross, R. Grywacz, J. H. Hamilton, M. Karmy, A. Fijalkowska, S. H. Liu, K. Miernik, S. W. Padgett, et al., *Phys. Rev. C* **89**, 054321 (2014).
- [42] T. Kautzsch, W. B. Walters, M. Hannawald, K.-L. Kratz, V. I. Mishin, V. N. Fedoseyev, W. Böhmer, Y. Jading, P. Van Duppen, B. Pfeiffer, et al., *Eur. Phys. J. A* **9**, 201 (2000).
- [43] N. Hoteling, W. B. Walters, B. E. Tomlin, P. F. Mantica, J. Pereira, A. Becerril, T. Fleckenstein, A. A. Hecht, G. Lorusso, M. Quinn, et al., *Phys. Rev. C* **76**, 044324 (2007).
- [44] L. Cáceres, M. Górska, A. Jungclaus, M. Pfützner, H. Grawe, F. Nowacki, K. Sieja, S. Pietri, D. Rudolph, Z. Podolyák, et al., *Phys. Rev. C* **79**, 011301 (2009).

- [45] A. Jungclaus, L. Cáceres, M. Górska, M. Pfützner, S. Pietri, E. Werner-Malento, H. Grawe, K. Langanke, G. Martínez-Pinedo, F. Nowacki, et al., *Phys. Rev. Lett.* **99**, 132501 (2007).
- [46] H.-K. Wang, K. Kaneko, and Y. Sun, *Phys. Rev. C* **89**, 064311 (2014).
- [47] M. Breitenfeldt, C. Borgmann, G. Audi, S. Baruah, D. Beck, K. Blaum, C. Böhm, R. B. Cakirli, R. F. Casten, P. Delahaye, et al., *Phys. Rev. C* **81**, 034313 (2010).
- [48] I. Dillmann, K.-L. Kratz, A. Wöhr, O. Arndt, B. A. Brown, P. Hoff, M. Hjorth-Jensen, U. Köster, A. N. Ostrowski, B. Pfeiffer, et al., *Phys. Rev. Lett.* **91**, 162503 (2003).
- [49] D. T. Yordanov, D. L. Balabanski, J. Bieroń, M. L. Bissell, K. Blaum, I. Budinčević, S. Fritzsche, N. Frömmgen, G. Georgiev, C. Geppert, et al., *Phys. Rev. Lett.* **110**, 192501 (2013).
- [50] R. F. Casten, J. Jolie, H. G. Borner, D. S. Brenner, N. V. Zamfir, W. T. Chou, and A. Aprahamian, *Phys. Lett. B* **297**, 19 (1992).
- [51] M. Déléze, S. Drissi, J. Jolie, J. Kern, and J. P. Vorlet, *Nucl. Phys. A* **554**, 1 (1993).
- [52] M. Bertschy, S. Drissi, P. E. Garrett, J. Jolie, J. Kern, S. J. Mannanal, J. P. Vorlet, N. Warr, and J. Suhonen, *Phys. Rev. C* **51**, 103 and **C52**, 1148 (1995).
- [53] H. Lehmann, P. E. Garrett, J. Jolie, C. A. McGrath, M. Yeh, and S. W. Yates, *Phys. Lett. B* **387**, 259 (1996).
- [54] N. Warr, S. Drissi, P. E. Garrett, J. Jolie, J. Kern, S. J. Mannanal, J.-L. Schenker, and J. P. Vorlet, *Nucl. Phys. A* **620**, 127 (1997).
- [55] P. E. Garrett, H. Lehmann, J. Jolie, C. A. McGrath, M. Yeh, and S. W. Yates, *Phys. Rev. C* **59**, 2455 (1999).
- [56] H. Lehmann, A. Nord, A. E. De Almeida Pinto, O. Beck, J. Besserer, P. von Brentano, S. Drissi, T. Eckert, R.-D. Herzberg, D. Jager, et al., *Phys. Rev. C* **60**, 024308 (1999).
- [57] F. Corminboeuf, T. B. Brown, L. Genilloud, C. D. Hanant, J. Jolie, J. Kern, N. Warr, and S. W. Yates, *Phys. Rev. Lett.* **84**, 4060 (2000).
- [58] F. Corminboeuf, T. B. Brown, L. Genilloud, C. D. Hanant, J. Jolie, J. Kern, N. Warr, and S. W. Yates, *Phys. Rev. C* **63**, 014305 (2000).
- [59] P. E. Garrett, H. Lehmann, J. Jolie, C. A. McGrath, M. Yeh, W. Younes, and S. W. Yates, *Phys. Rev. C* **64**, 024316 (2001).
- [60] A. Gade, J. Jolie, and P. von Brentano, *Phys. Rev. C* **65**, 041305(R) (2002).
- [61] A. Gade, A. Fitzler, C. Fransen, J. Jolie, S. Kasemann, H. Klein, A. Linnemann, V. Werner, and P. von Brentano, *Phys. Rev. C* **66**, 034311 (2002).
- [62] C. Kohstall, D. Belic, P. von Brentano, C. Fransen, A. Gade, R.-D. Herzberg, J. Jolie, U. Kneissl, A. Linnemann, A. Nord, et al., *Phys. Rev. C* **72**, 034302 (2005).
- [63] A. Linnemann, C. Fransen, J. Jolie, U. Kneissl, P. Knoch, C. Kohstall, D. Mücher, H. H. Pitz, M. Scheck, C. Scholl, et al., *Phys. Rev. C* **75**, 024310 (2007).
- [64] M. Déléze, S. Drissi, J. Kern, P. A. Tercier, and J. P. Vorlet, *Nucl. Phys. A* **551**, 269 (1993).
- [65] P. E. Garrett and J. L. Wood, *J. Phys. G* **37**, 064028, and corrigendum 06970128 (2010).
- [66] K. L. G. Heyde and J. L. Wood, *Rev. Mod. Phys.* **83**, 1467 (2011).
- [67] National Nuclear Data Center (NNDC), Brookhaven National Laboratory, <http://www.nndc.bnl.gov/ensdf/> (May 2016).
- [68] T. Faestermann, M. Górska, and H. Grawe, *Prog. Part. Nucl. Phys.* **69**, 85 (2013).
- [69] B. A. Brown and K. Rykaczewski, *Phys. Rev. C* **50**, R2270 (1994).
- [70] K. L. G. Heyde, C. De Coster, J. Jolie, and J. L. Wood, *Phys. Rev. C* **46**, 541 (1992).
- [71] J. Jolie and H. Lehmann, *Phys. Lett. B* **342**, 1 (1995).
- [72] K. L. G. Heyde, J. Jolie, H. Lehmann, C. De Coster, and J. L. Wood, *Nucl. Phys. A* **586**, 1 (1995).
- [73] H. Lehmann and J. Jolie, *Nucl. Phys. A* **588**, 623 (1995).
- [74] C. De Coster, K. L. G. Heyde, B. Decroix, P. Van Isacker, J. Jolie, H. Lehmann, and J. L. Wood, *Nucl. Phys. A* **600**, 251 (1996).
- [75] H. Lehmann, J. Jolie, C. De Coster, B. Decroix, K. L. G. Heyde, and J. L. Wood, *Nucl. Phys. A* **621**, 767 (1997).
- [76] C. De Coster, B. Decroix, K. L. G. Heyde, J. L. Wood, J. Jolie, and H. Lehmann, *Nucl. Phys. A* **621**, 802 (1997).
- [77] C. De Coster, B. Decroix, K. L. G. Heyde, J. Jolie, H. Lehmann, and J. L. Wood, *Nucl. Phys. A* **651**, 31 (1999).
- [78] L. Prochniak, P. Quentin, and M. Imadalou, *Mod. Phys. E* **21**, 1250036 (2012).
- [79] T. R. Rodriguez, J. L. Egido, and A. Jungclaus, *Phys. Lett. B* **668**, 410 (2008).
- [80] K. Kumar, *Phys. Rev. Letters* **28**, 249 (1972).
- [81] D. Cline, *Annu. Rev. Nucl. Part. Sci.* **36**, 683 (1986).
- [82] D. Cline, in *Proc. of the Orsay Colloquium on Intermediate Nuclei*, edited by R. Foucher (Orsay Inst. Phys. Nucl., 4, 1971).
- [83] D. Cline and C. Flaum, in *Proc. of Int. Conf. on Nuclear Structure using Electron Scattering*, edited by K. Shoda and H. Ui (Sendai 1972, Sendai, Tohoku Univ. 61, 1972).
- [84] D. Cline, in *Proc. of the Int. Conf. on Interacting Bose-Fermi systems in Nuclei*, edited by F. Iachello (Plenum Press, New-York, 241, 1983).
- [85] A. Bohr and B. Mottelson, *Nuclear Structure Vol. II: Nuclear Deformation* (World Scientific Publishing, 1998).
- [86] A. Holt, T. Engeland, M. Hjorth-Jensen, and E. Osnes, *Phys. Rev. C* **61**, 064318 (2000).
- [87] B. A. Brown, P. M. S. Lesser, and D. B. Fossan, *Phys. Rev. C* **13**, 1900 (1976).
- [88] K. Sieja, F. Nowacki, K. Langanke, and G. Martínez-Pinedo, *Phys. Rev. C* **79**, 064310 (2009).
- [89] A. Blazhev, K. L. G. Heyde, J. Jolie, and T. Schmidt, *Proc. of the CGS15 conference*, EPJ Web of Conferences **93**, 01016 (2015).
- [90] A. D. Ayangeakaa, R. V. F. Janssens, C. Y. Wu, J. M. Allmond, J. L. Wood, S. Zhu, M. Albers, S. Almaraz-Calderon, B. Bucher, M. P. Carpenter, et al., *Phys. Lett. B* **754**, 254 (2014).
- [91] A. Górgen and W. Korten, *J. Phys. G* **43**, 024002 (2016).
- [92] E. Clément, A. Górgen, W. Korten, E. Bouchez, A. Chatillon, J.-P. Delaroche, M. Girod, H. Goutte, A. Hürstel, Y. Le Coz, et al., *Phys. Rev. C* **75**, 054313 (2007).
- [93] K. Wrzosek-Lipska, L. Próchniak, M. Zielińska, J. Srebrny, K. Hadyńska-Klęk, J. Iwanicki, M. Kisieliński, M. Kowalczyk, P. J. Napiorkowski, D. Piętak, et al., *Phys. Rev. C* **86**, 064305 (2012).
- [94] J. Srebrny, T. Czosnyka, C. Droste, S. Rohoziński, L. Próchniak, K. Zajac, K. Pomorski, D. Cline, C. Y.

- Wu, A. Bäcklin, et al., Nucl. Phys. A **766**, 2551 (2006).
- [95] J. Srebrny and D. Cline, Int. J. Mod. Phys. E **20**, 422 (2011).
- [96] C. Y. Wu, D. Cline, E. G. Vogt, W. J. Kernan, T. Czosnyka, K. G. Helmer, R. W. Ibbotson, A. E. Kavka, B. Kotlinski, and R. M. Diamond, Nucl. Phys. A **533**, 359 (1991).
- [97] C. Y. Wu, D. Cline, T. Czosnyka, A. Backlin, C. Baktash, R. M. Diamond, G. D. Dracoulis, L. Hasselgren, H. Kluge, B. Kotlinski, et al., Nucl. Phys. A **607**, 178 (1996).
- [98] N. Bree, K. Wrzosek-Lipska, A. Petts, A. Andreyev, B. Bastin, M. Bender, A. Blazhev, B. Bruyneel, P. A. Butler, J. Butterworth, et al., Phys. Rev. Lett. **112**, 162701 (2014).
- [99] N. Kesteloot, B. Bastin, L. P. Gaffney, K. Wrzosek-Lipska, K. Auranen, C. Bauer, M. Bender, V. Bildstein, A. Blazhev, S. Bönig, et al., Phys. Rev. C **92**, 054301 (2015).
- [100] J. E. García-Ramos and K. L. G. Heyde, Phys. Rev. C **89**, 014306 (2014).
- [101] J. E. García-Ramos and K. L. G. Heyde, Phys. Rev. C **92**, 034309 (2015).
- [102] R. V. Jolos, P. von Brentano, N. Pietralla, and I. Schneider, Nucl. Phys. A **618**, 126 (1997).
- [103] V. Werner, E. Williams, R. J. Casperson, R. F. Casten, C. Scholl, and P. von Brentano, Phys. Rev. C **78**, 051303(R) (2008).
- [104] J. Dobaczewski, S. G. Rohozinski, and J. Srebrny, Nucl. Phys. A **462**, 72 (1987).
- [105] M. Borge, Nucl. Instrum. Methods Phys. Res., Sect. B **376**, 408 (2016).
- [106] S. G. Nilsson, Kon. Dan. Vidensk Selsk. Mat. Fys. Medd. **29**, n16 (1955).
- [107] S. G. Nilsson and I. Ragnarsson, *Nuclear Shells and Shapes* (Cambridge Univ. Press, New-York, 1995).
- [108] L. Próchniak and S. G. Rohozinski, J. Phys. G **36**, 123101 (2009).
- [109] J. Eisenberg and W. Greiner, *Nuclear Theory Vol. 1 - Nuclear Models* (North-Holland Physics Publishing, 1987).
- [110] N. Pietralla, P. von Brentano, R. F. Casten, T. Otsuka, and N. V. Zamfir, Phys. Rev. Lett. **73**, 2962 (1994).
- [111] R. F. Casten, *Nuclear Structure from a Simple Perspective* (Oxford University Press, 2005).
- [112] I. Thorslund, C. Fahlander, J. Nyberg, S. Juutinen, R. Julin, M. Piiparinen, R. Wyss, A. Lampinen, T. Lönnroth, D. Müller, et al., Nucl. Phys. A **564**, 285 (1993).
- [113] A. P. Zuker, J. Retamosa, A. Poves, and E. Caurier, Phys. Rev. C **52**, R1741(R) (1995).
- [114] G. Martínez-Pinedo, A. P. Zuker, A. Poves, and E. Caurier, Phys. Rev. C **55**, 187 (1997).
- [115] A. Arima, M. Harvey, and K. Shimizu, Phys. Lett. B **30**, 517 (1969).
- [116] K. Hecht and A. Adler, Nucl. Phys. A **137**, 129 (1969).
- [117] J. P. Elliott, Proc. Roy. Soc. A **245**, 128 (1958).
- [118] J. P. Elliott, Proc. Roy. Soc. A **254**, 562 (1958).
- [119] J. Duflo and A. P. Zuker, Phys. Rev. C **59**, R2347(R) (1999).
- [120] F. Nowacki, Acta Phys. Pol. B **38**, 1369 (2007).
- [121] J. Phys. G **43**, focus section 020401 (2016).
- [122] N. Benczer-Koller, G. J. Kumbartzki, K.-H. Speidel, D. A. Torres, S. J. Q. Robinson, Y. Y. Sharon, J. M. Allmond, P. Fallon, I. Abramovic, L. A. Bernstein, et al., Phys. Rev. C **94**, 034303 (2016).